Journal of Natural Gas Science and Engineering 28 (2016) 434–446

Contents lists available at ScienceDirect

Journal of Natural Gas Science and Engineering

journal homepage: www.elsevier.com/locate/jngse

Organic matter properties and shale gas potential of Paleozoic shales in Sichuan Basin, China

Jincai Tuo, Chenjun Wu*, Mingfeng Zhang

Key Laboratory of Petroleum Resources, Gansu Province/ Key Laboratory of Petroleum Resources Research, Institute of Geology and Geophysics, Chinese Academy of Sciences, Lanzhou 730000, PR China

ARTICLE INFO

Article history:
Received 2 September 2015
Received in revised form
30 November 2015
Accepted 6 December 2015
Available online 12 December 2015

Keywords:
Sichuan basin
Shale gas
Marine shale
Organic matter
Overmature source rocks
Biomarkers

ABSTRACT

In this study, Lower Paleozoic shale samples collected from Lower Cambrian Niutitang Formation, Upper Ordovician Wufeng Formation, and Lower Silurian Longmaxi Formation in different regions in the Sichuan Basin were analyzed using geochemical and petrophysical methods to characterize the difference in organic matter properties (including abundance, type and thermal maturity), pore development, mineralogy to shale gas resources potential. The studied marine shales all displayed excellent, high-quality organic matter richness and could be the strata for shale gas generation over geological time. There are four systematic geochemical and petrophysical variation trends that indicate that the overmature source rocks of the Sichuan Basin constitute a special shale gas reservoir system: (1) The measured $\delta^{13}C$ values for sedimentary organic carbon (TOC) presents a distinct trend indicative of ^{13}C enrichment, which indicates that the TOC may be related to the diversity of preserved phytoplankton in the different shale strata in the Sichuan Basin. This biont diversity and organism replacement process were confirmed by the biomarker distribution patterns in the sediments. (2) The bitumen "A" contents display negative correlation with sedimentary age and TOC, suggesting that most of the residual liquid hydrocarbons in those shales have been transformed into shale gas due to higher thermal maturity during the diagenetic transformation of the organic matter burial process, and the shale gas in reservoirs in those types of shales were mostly generated from the cracking of residual bitumen during a stage of relatively high thermal evolution. (3) The quartz and TOC present strongly positive relationship, suggesting that the increased quartz in most of the marine shales is a biogenic silica signal. (4) Total porosity displays a negative relationship with TOC and the quartz contents in the three Paleozoic marine shales, suggesting that re-precipitated pyrobitumen created by oil cracked to gas in overmature source rocks could be the reason leading to the lowest porosity and smaller pores in the most aged but most TOC-abundant shales. Skewing toward smaller pores will reduce the pore volume and result in larger internal surface areas and greater sorption energies, which should reduce the productive capacity of shale gas.

1. Introduction

Shale gas is an unconventional gas system in which shale is both the source of and the reservoir for natural gases that are derived from organic matter within the shale through biogenic and/or thermogenic processes (Curtis, 2002; Hill et al., 2007; Loucks and Ruppel, 2007; Strąpoć et al., 2010; Zhang et al., 2014). Unconventional shale gas has evolved into an important resource play for the United States, accounting for approximately 23% of the produced gas in the United States by the end of 2011 (Hao et al., 2013). China is one country that is relatively rich in shale gas resources. Recoverable shale gas resources are predicted to be approximately 26×10^{12} m^3 in China (Zhang et al., 2011), which is close to the 28×10^{12} m^3 in the USA, and approximately 58% of those shale gas resources are predicted to be stored in Paleozoic shales in southern China. There are three regionally developed black shales that are considered to be favorable for shale gas resource exploration and development: the black shales of the Niutitang Formation, Lower Cambrian; and the Wufeng-Longmaxi Formations, Upper Ordovician-Lower Silurian, which were deposited in marine facies (Zhang et al., 2008; Hao and Zhou., 2013; Hao et al., 2013; Zou et al., 2014). The organic matter in most of those black shales is

* Corresponding author.
E-mail address: wcj627@lzb.ac.cn (C. Wu).

http://dx.doi.org/10.1016/j.jngse.2015.12.003
1875-5100/

considered to be in the highly mature or post-mature gas-generating stages (usually Ro > 2.5%), which are favorable for shale gas generation (Huang et al., 1996; Zhu et al., 2006; Zhou et al., 2014). Overmature, organic-rich shales exhibit high degrees of organic matter conversion and therefore have good potential to exhibit high gas contents and high gas flow rates (Jarvie et al., 2007).

The Sichuan Basin is now regarded as the most promising region in southern China for making a breakthrough in shale gas resource exploration and development in the near future. The shale distribution regularities, geological conditions for gas pool formation, hydrocarbon accumulation mechanisms and gas resource assessment in the Sichuan Basin have been widely and intensively studied (Dai et al., 2001; Zhang et al., 2004; Ma et al., 2004; Tenger et al., 2007; Wang et al., 2009; Nie et al., 2009, 2011; Zhu et al., 2010; Chen et al., 2011). In this study, we selected five vertical profiles which covered three Paleozoic strata and conducted geochemical analysis, mineralogy and porosity measurement. We have compared the organic matter properties, lithology and pore development for three strata of the Paleozoic shale, Sichuan Basin, China. The main objectives of this study are to: (1) evaluate the main controls on the variation of organic matter, including abundance, type and thermal maturation; (2) compare the mineralogy and lithology among three strata; (3) determine the key controls to shale gas reservoir properties; and (4) evaluate the shale gas potential of Paleozoic shale. Our experimental findings have important implications for shale gas storage, resource assessments and shale gas potential prediction.

2. Distribution of shales in the Sichuan Basin

According to a previous study (Liang et al., 2009), there are three black shale strata that can be assumed to be the potential source rocks for oil and gas resources developed in the Sichuan Basin. These strata are, from the lower to upper layers, Lower Cambrian, Upper Ordovician, and Lower Silurian. The Niutitang Formation (also called the Qiongzhusi Formation and Jiulaodong Formation in the southwestern part of the Sichuan Basin), Lower Cambrian; the Wufeng Formation, Upper Ordovician; and the Longmaxi Formation, Lower Silurian, are three regionally developed high-quality black shales in the Sichuan Basin.

The black shale of the Niutitang Formation, Lower Cambrian, is widely distributed throughout nearly all of the Sichuan Basin except in the Chuanzhong paleohigh. The shale has multiple depocenters with sedimentary thickness ranging from 300 to 500 m and thickening to the south and east. The black shale of the Wufeng Formation, Upper Ordovician, is typically less than 20 m in thickness. The black shale of the Longmaxi Formation, Lower Silurian, is widely distributed throughout the Sichuan Basin. This shale can be detected in the eastern and southern areas of the Leshan-Longnvsi paleohigh, although it has been subject to denudation in the paleohigh area. There are three superior Lower Silurian areas of source rock development, including Zhenba-Guanyin, Yunyang-Shizhu-Guanyinqiao and Yibin-Luzhou. The maximum thickness of the Longmaxi Formation, Lower Silurian, is in the range of 500–1250 m (Zou et al., 2010).

3. Materials and methods

3.1. Samples

The shale samples examined in this study were collected from both outcrops and drilling cores, including the Youyang Cambrian outcrop profile, the ZK-909 Cambrian drill well, the Changning and Xingwen Upper Ordovician-Lower Silurian outcrop profile, and the Qianqian-1 Upper Ordovician-Lower Silurian drill well (Fig. 1). Sampling information are shown on Table 1. The Youyang Cambrian outcrop profile is located in Tonglin village, Youyang County, southeastern Sichuan Basin. Thirty black shale samples were collected from this 30-m-thick outcrop profile. The ZK-909 well is located in Kaiyang County, southern Sichuan Basin, and the Lower Cambrian strata were drilled to depths of 211.8 m–413.56 m, in which 166 shale samples were collected. The Changing and Xingwen Upper Ordovician-Lower Silurian profile are located in Changning County in the southern part of the Sichuan Basin, with thickness of 93.1 m and 63 m respectively. The Qianqian-1 well is located in Qianjiang District, approximately 200 km southeast of Chongqing City, and the Upper Ordovician-Lower Silurian strata were drilled to depths of 695.86 m–798.65 m. A total of 144 outcrop and 58 core samples were collected in Ordovician-Lower Silurian strata (Table 1). All of the samples collected from outcrop profiles were obtained in the area adjacent to newly constructed roads (e.g., the Changning and Xingwen Upper Ordovician-Lower Silurian outcrop profile) or in new quarries and open-pit mining areas (e.g., the Youyang Cambrian outcrop profile), ensuring that the lithological and geochemical characteristics of these fresh samples were not affected by the weathering conditions.

3.2. Experimental

Total organic carbon (TOC) was determined for pulverized sediments; carbonates were removed by treating the samples with 8% hydrochloric acid, and organic carbon was determined by LECO-CS344 analyses. The $\delta^{13}C$ value of the TOC was determined using another decalcified aliquot by combusting it to release CO_2, which was then injected into a Finnigan MAT 252 mass spectrometer.

Based on the TOC and $\delta^{13}C$ characteristics, samples were further selected for soluble organic matter extraction and GC–MS analyses. The selected shale samples were powdered to a particle size less than 120 mesh and Soxhlet-extracted with chloroform for 72 h. Because the organic matter in most of the shale samples was in a highly mature or post-mature phase, we only obtained trace amounts (ppm level) of soluble organic matter; therefore, we did not attempt to separate the extracts into subfractions.

GC–MS analyses of soluble extracts were performed on a Hewlett–Packard 5890II gas chromatograph interfaced with a Hewlett–Packard 5989 A mass spectrometer. The gas chromatograph was equipped with a HP-5 fused-silica capillary column (30 m × 0.32 mm), and He was used as a carrier gas with a flow rate of 1 ml/min. The mass spectrometer was operated at an electron energy of 70 eV and ion source temperature of 250 °C. The oven temperature was programmed to increase from 80 to 200 °C at 4 °C/min and then from 200 to 300 °C at 3 °C/min. The GC–MS data were acquired and processed with a Hewlett–Packard Chemstation data system.

The porosity and pore diameter distribution were determined from 20 selected shales processed using a micro nuclear magnetic resonance instrument. The instrument was a MicroMR02-025V NM2, with a resonant frequency of 2.18 MHz, probe coil diameter of 25 mm and magnetic body temperature of 32 ± 0.01 °C. The relative repeatability standard deviation for porosity was less than 4.3%. The FE-SEM imaging of nanopores was performed on the surfaces prepared by Ar ion milling (IM4000, Hitachi High-Tech) using an accelerating voltage of 3 kV and a milling time of 3 h.

4. Results and discussion

4.1. Characteristics of organic matter

4.1.1. Total organic carbon (TOC)

The characteristics of organic matter (richness, type and maturity) are believed to be some of the most important properties

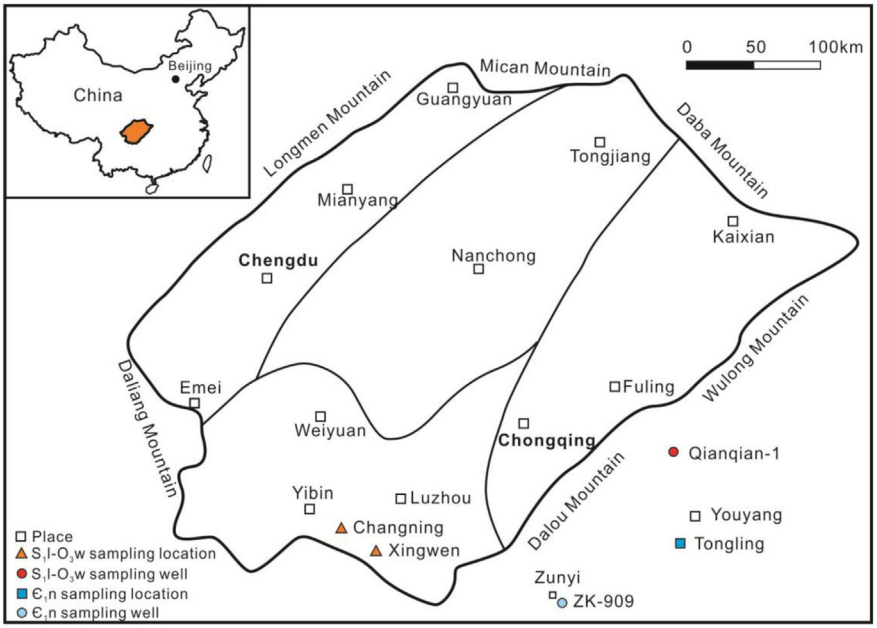

Fig. 1. Map showing the locations of the Sichuan Basin and sampling area.

Table 1
Sampling information, TOC, and $\delta^{13}C_{TOC}$ of Paleozoic shales in Sichuan Basin.

Profile	Strata	Thickness (m)			Average sampling Intervals (m)	N	TOC (%) Min ~ Max/Avg	$\delta^{13}C_{TOC}$ (‰) Min ~ Max/Avg
		Total	1.0% ≤ TOC<2.0%	TOC≥2.0%				
Xingwen	S_1l	55.5	35	10	1.46	38	0.83–3.32/1.43	−30.9~-28.8/-29.9
	O_3w	7.5	2	5.5	1.25	6	1.74–4.54/3.56	−30.6~-30.2/-30.4
Changning	S_1l	83.1	40.6	37.5	1	80	0.81–7.28/1.97	−31.2~-29.4/-30.1
	O_3w	10	0.5	9	0.5	20	0.77–7.76/3.53	−30.8~-29.5/-30.3
Qianqian-1	S_1l	93.51	56.39	16.44	1.8	51	0.15–4.64/1.29	−31.4~-26.6/-29.7
	O_3w	9.28	1.2	4.36	1.5	7	0.01–6.09/2.54	−31.4~-28.3/-30.4
ZK-909	$Є_1n$	201.76	28.7	71.06	1.2	166	0.11–6.67/2.11	−34.3~-27.4/-32.2
Youyang	$Є_1n$	30	0	30	1	30	2.42–12.9/7.85	−32.4~-31.1/-31.8

N: Number of collected samples.

controlling gas generation and storage capacity in shales (Hao et al., 2013). Excellent original organic richness and generation potential have resulted in the production of large amounts of gas in key productive areas of the Barnett Shale of the Fort Worth Basin, Texas (Jarvie et al., 2007). The analyzed Paleozoic shales in the Sichuan Basin all display excellent, high-quality organic matter richness features (Table 1). The measured total organic carbon (TOC) for all 196 Lower Cambrian shale samples ranged from 0.11 to 12.9%, with an average of 2.99%, and 60.2% of the Lower Cambrian shales exhibit a TOC>2%. Total organic matter distribution of shale samples from Youyang Cambrian outcrop profile and the ZK-909 Cambrian drill well are shown on Fig. 2a and Fig. 2b. TOC for all Upper Ordovician shale samples ranged from 0.01 to 7.76%, with an average of 3.33%, and 81.8% of the Upper Ordovician shales exhibit a TOC>2%. TOC for all Lower Silurian shale samples ranged from 0.15 to 7.28%, with an average of 1.64%, and organic rich shales with TOC larger than 1% and 2% accounted for 17.2% and 82.2% respectively. All of these organic matter properties suggest that the Niutitang and Wufeng-Longmaxi black shales have demonstrated excellent, high-quality organic matter richness for shale gas generation over geological time.

4.1.2. $\delta^{13}C$ of TOC

The carbon isotopic composition of living organisms varies as a function of environmental conditions, and therefore, the isotope analysis of sedimentary organic carbon is often used for paleoenvironmental reconstructions (Popp et al., 1997; Dawson et al., 2002). Variations in the carbon isotopic composition of marine organic matter have also been used for chemostratigraphic correlations (Knoll et al., 1986; Kaufman et al., 1991) as well as environmental interpretations (Arthur et al., 1985; Dean et al., 1986; Hayes et al., 1989). The carbon isotopic compositions for the sedimentary organic carbon (TOC) in the three black shale strata in the Sichuan Basin display characteristic differences in the carbon isotopic values. The measured $\delta^{13}C$ values for the sedimentary organic carbon in the three black shale strata in the Sichuan Basin present a distinct trend of ^{13}C enrichment (Fig. 3, Table 1). Compared with the lower Cambrian shales, upper Ordovician shales and lower Silurian shales, either TOC less than 2.0% (Fig. 3a) or greater than 2.0% (Fig. 3b), all display a trend of ^{13}C enrichment. This trend is completely opposite of the trend of the thermal evolution of sedimentary organic matter, which usually displays a trend of ^{13}C enrichment with burial depth because the breaking-down of kerogen during catagenesis involves the splitting of various types of bonds and the release of smaller molecules (isotopically lighter), which leads to residual sedimentary organic matter rich in ^{13}C (Tissot and Welte, 1984). The comparison of evolutionary changes in the different black shale strata with respect to the carbon isotopic composition for the sedimentary organic carbon suggests that isotopic shifts of TOC may generally be related to the types and

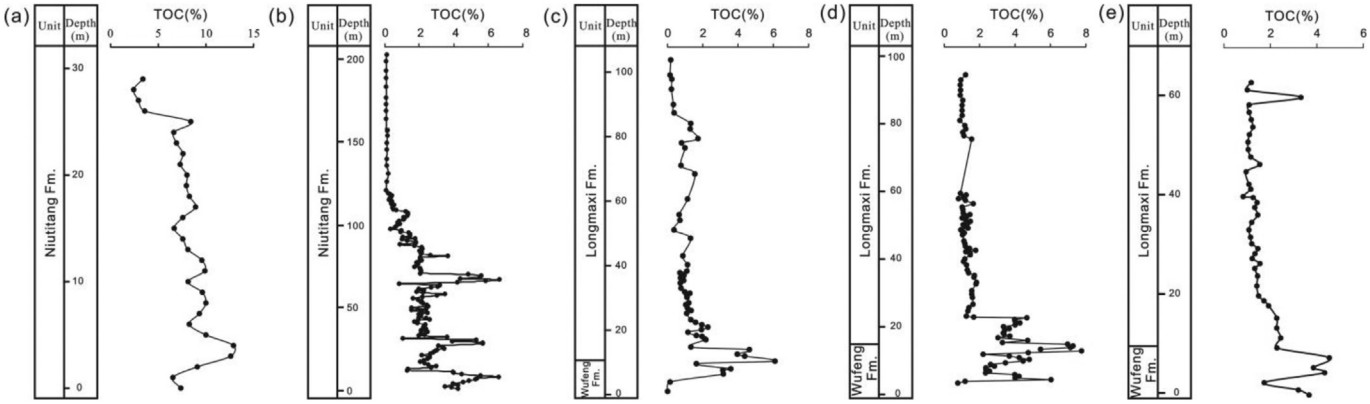

Fig. 2. Comparision show the vertical variation of TOC (%) for the 5 sampling profiles: (a) Youyang Cambrian outcrop profile, (b) ZK-909 well Cambrian drill well, (c) Qianqian-1 well Upper Ordovician-Lower Silurian drill well, (d) Changning Upper Ordovician-Lower Silurian outcrop profile, (e) Xingwen Upper Ordovician-Lower Silurian outcrop profile.

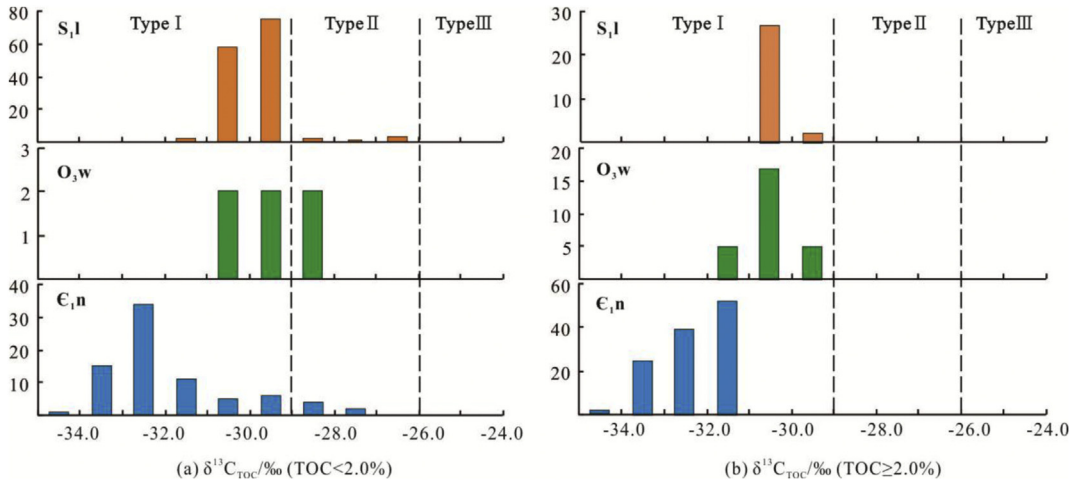

Fig. 3. Comparison of the variation trends of $\delta^{13}C$ and ^{13}C components of TOC in different strata. (a) The organic carbon isotopic compositions for samples with TOC less than 2.0%. (b) The organic carbon isotopic compositions for samples with TOC greater than 2.0%.

diversity of preserved phytoplankton in the different shale strata in the Sichuan Basin. The sedimentary organic carbon (TOC) in the lower Cambrian (Niutitang Formation) shales exhibit the lightest carbon isotopic composition, with an average $\delta^{13}C$ value of −32.2‰, and the greatest homogenous variation (range = 6.9‰). The TOC in the upper Ordovician (Wufeng Formation) shales and lower Silurian (Longmaxi Formation) shales have carbon isotopic compositions heavier than those of the Lower Cambrian Niutitang, with average $\delta^{13}C$ values of −30.3‰ (range = 3.1‰) and −29.9‰ (range = 4.6‰), respectively.

The presence and absence of a mineral skeleton has been suggested to be a principal factor controlling the $\delta^{13}C$ values of sedimentary organic matter during diagenesis (Andrusevich et al., 1998), assuming one of two pathways: sapropel-type diagenesis or humus-type diagenesis (Kodina and Galimov, 1985). In the first case, the organic matter was enriched in more resistant, isotopically depleted lipids because microorganisms consumed the proteins and carbohydrates of organic-walled phytoplankton (dominant in the Precambrian and early Cambrian). This process explains why the sedimentary organic carbons (TOC) in the Lower Cambrian (Niutitang Formation) shales have the lightest carbon isotopic composition. In contrast, humus-type diagenesis occurring in phytoplankton with calcareous or siliceous tests (which dominated in the Mesozoic and Cenozoic) and terrigenous vegetal debris (which are assumed to start from the middle Silurian, Edwards et al., 1992; Kenrick and Crane, 1997) involve carbohydrate-protein and lignin-cellulose complexes protected by mineralized skeletons. Greater preservation of the organic matter of marine phytoplankton may have occurred when dominantly organic-walled phytoplankton (blue-green algae, acritarchs) were replaced by mainly calcareous-walled organisms (coccolithophorids and dinoflagellates). The latter types are known to have existed since the Silurian but did not flourish until the post-Triassic period. Therefore, it is significant that the $\delta^{13}C$ values of the organic matter in the upper Ordovician (Wufeng Formation) shales and lower Silurian (Longmaxi Formation) shales are heavier than those of Lower Cambrian (Niutitang Formation) shales. The carbon isotopic composition of the TOC in the three black shale strata in the Sichuan Basin suggest that the organic matter in Lower Paleozoic marine shales constituted a sapropelic, oil-prone source, and the shale gas (if any) stored in reservoirs in those types of shales was mostly generated from the cracking of residual bitumen during a stage of relatively high thermal evolution. This has been confirmed by some latest research (e.g. Zou et al., 2015; Dai et al., 2014).

4.1.3. Soluble organic matter

According to previous studies, the organic matter in most black shales in the Sichuan Basin are considered to be in highly mature or post-mature gas-generating stages (usually in the Ro>2.5% stage) (Zhang et al., 2008; Hao and Zhou, 2013; Hao et al., 2013). Although

Table 2
Bitumen"A" content statistics results in the 3 lower Paleozoic marine strata.

Strata	Lithology	TOC(%)		Bitumen"A"[a](ppm)		Bitumen"A"/TOC([a]10^{-4})	
		Range	Average	Range	Average	Range	Average
Lower Silurian	Shale	0.92–1.8	1.35	17–34	26	13.9–30.9	20.1
Upper Ordovician	Shale	2.56–4.75	3.7	6–17	13	1.5–4.9	3.5
Lower Cambrian	Shale	2.42–9.89	7.85	7–19	11	0.73–13.7	1.89

[a] Bitumen"A" = chloroform soluble extract.

most of those Paleozoic marine shales are rich in TOC, and the organic matter in those shales is a type of oil-prone source material, they contain hardly any or only very low amounts of soluble organic matter (Table 2). The measured soluble organic matter (bitumen "A") for the 37 selected marine shale samples (TOC ranges from 0.92 to 9.89%) range from 6 to 34 ppm (Table 2). The bitumen "A" content and the relative content of bitumen "A"/TOC are selected parameters that are typically used to describe how much and what relative portion of total organic matter (TOC) can be transformed into soluble organic matter in a specific source rock. In the plots of bitumen "A" and bitumen "A"/TOC versus TOC, different types of Paleozoic marine shales can be clearly differentiated (Fig. 4). The lower Silurian (Longmaxi Formation) shales show relatively higher bitumen "A" and bitumen "A"/TOC contents, whereas the Lower Cambrian (Niutitang Formation) shales show lower bitumen "A" and bitumen "A"/TOC contents. The three Paleozoic marine shale strata in the Sichuan Basin present distinct trends decreasing bitumen "A" and bitumen "A"/TOC with increasing age. Interestingly, those trends indicate a negative correlation between bitumen "A" and bitumen "A"/TOC with increases in TOC (Fig. 4). This visually contradictory phenomenon (the greater the level of TOC, the lower the bitumen "A" content in the shales) suggests that most of the residual liquid hydrocarbons in those shales have been transformed into shale gas because of the higher thermal maturity of organic matter burial during diagenetic transformation (Xia et al., 2013; Xia, 2014) such that the shale gas (if any) stored in reservoirs in those types of shales was mostly generated from the cracking of residual bitumen during a stage of relatively high thermal evolution.

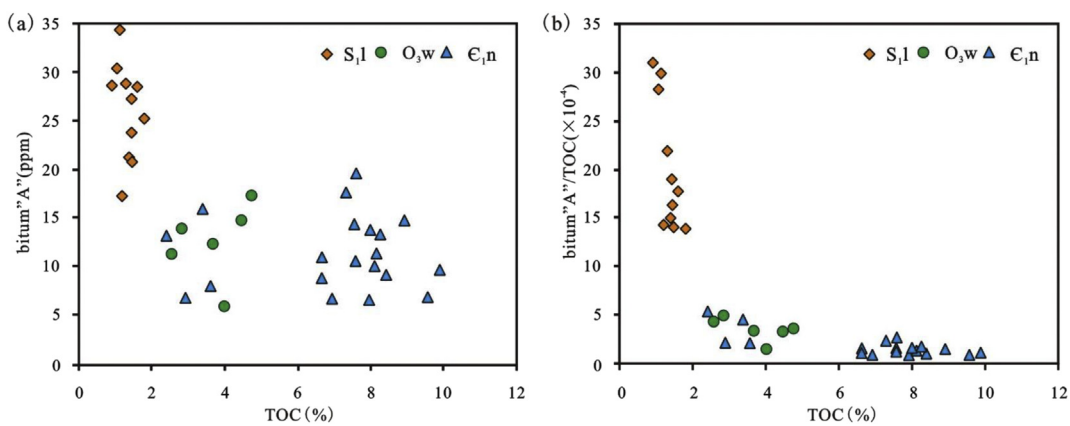

Fig. 4. Plots of bitumen "A" and bitumen "A"/TOC versus TOC.

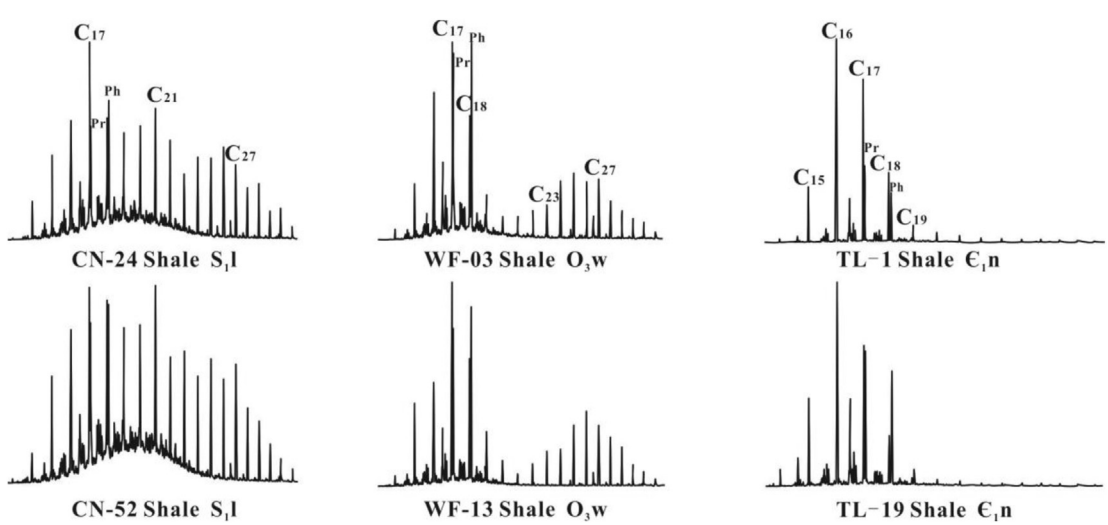

Fig. 5. Comparison of the distributions of paraffins in different strata.

Table 3
Parameters for the three series of biomarker compounds detected in the samples from 3 potential shale gas strata in Sichuan basin, China.

Sample no.	Strata	Lithology[a]	TOC(%)	$\delta^{13}C_{TOC}$ (‰)	Paraffins					Terpenoids			Steranes					
					Cmax[b]	Pr/Ph	Pr/C_{17}	Ph/C_{18}	$\sum C_{21}^{-}/\sum C_{22}^{+}$[c]	Ts/Tm	$C_{23}tt$[d]/C30h	$C_{31}22S/(S+R)$	C_{27}(%)	C_{28}(%)	C_{29}(%)	$C_{29}\alpha\alpha 20S/(S+R)$	$C_{29}\beta\beta/(\alpha\alpha+\beta\beta)$	$C_{27}R/C_{29}R$
CN-22	S_1l	S	1.4	−30.3	C_{20}	0.65	0.84	1.98	3.13	0.66	6.20	0.55	39.04	27.78	33.18	0.36	0.31	0.71
CN-24	S_1l	S	1.6	−29.7	C_{16}	0.91	0.84	1.27	1.61	0.87	3.34	0.64	41.50	29.59	28.91	0.48	0.33	1.34
CN-27	S_1l	S	1.8	−29.7	C_{17}	0.79	0.69	1.29	1.87	0.76	5.43	0.66	45.75	25.48	28.77	0.44	0.32	1.43
CN-32	S_1l	S	1.31	−29.6	C_{18}	0.78	0.83	1.38	1.87	0.61	5.22	0.64	46.03	25.29	28.68	0.50	0.41	1.76
CN-40	S_1l	S	1.43	−30.0	C_{21}	0.84	0.64	1.18	2.19	0.64	7.09	0.67	48.16	24.66	27.18	0.43	0.33	1.45
CN-45	S_1l	S	1.14	−30.3	C_{17}	0.68	0.59	1.10	2.23	0.65	6.01	0.63	46.45	26.95	26.60	0.41	0.28	1.36
CN-50	S_1l	S	1.07	−29.7	C_{17}	0.70	0.53	1.26	2.43	0.69	9.38	0.65	45.46	27.20	27.33	0.44	0.34	1.57
CN-52	S_1l	S	1.48	−30.0	C_{16}	0.64	0.93	1.48	1.40	0.78	6.95	0.70	46.32	25.27	28.41	0.40	0.42	1.72
CN-56	S_1l	S	1.45	−29.7	C_{17}	0.88	0.97	1.60	1.47	0.83	5.95	0.60	41.72	25.53	32.75	0.39	0.38	1.21
CN-61	S_1l	S	1.2	−29.9	C_{17}	0.82	0.69	1.18	2.05	0.69	9.54	0.68	47.09	26.08	26.84	0.40	0.41	1.82
CN-65	S_1l	S	0.92	−30.0	C_{17}	0.70	0.78	1.67	1.79	0.80	7.11	0.67	42.03	28.91	29.06	0.45	0.39	1.39
WF-03	O_3w	S	4.93	−30.7	C_{16}	0.86	1.20	2.18	1.56	1.11	0.75	0.65	30.39	30.61	39.00	0.36	0.29	0.68
WF-07	O_3w	S	2.56	−30.7	C_{16}	0.84	0.89	1.56	1.27	1.17	0.76	0.60	30.91	30.76	38.33	0.40	0.31	0.81
WF-10	O_3w	S	2.84	−30.7	C_{17}	0.91	0.75	1.47	1.02	1.01	0.50	0.66	28.16	31.19	40.65	0.35	0.35	0.65
WF-13	O_3w	S	4.46	−29.9	C_{17}	0.80	0.99	2.11	1.33	0.90	1.13	0.65	30.95	31.93	37.12	0.33	0.38	0.74
WF-16	O_3w	S	3.68	−29.8	C_{16}	1.09	0.93	1.31	0.82	0.98	0.84	0.66	32.08	29.57	38.35	0.46	0.29	0.80
WF-18	O_3w	S	4.75	−30.3	C_{17}	0.63	0.63	1.66	0.67	1.44	0.49	0.64	30.73	30.40	38.87	0.40	0.29	0.66
TL-1	ϵ_1n	S	3.39	−31.1	C_{16}	1.57	0.66	1.08	35.49	0.64	0.32	0.59	27.59	29.75	42.66	0.43	0.37	0.61
TL-2	ϵ_1n	S	2.42	−31.5	C_{16}	1.36	0.6	1.08	65.2	0.69	0.31	0.57	28.65	33.53	37.82	0.48	0.35	0.72
TL-3	ϵ_1n	S	2.92	−31.7	C_{16}	1.57	0.8	1.25	36.71	1.04	0.23	0.61	30.8	26.88	42.32	0.48	0.38	0.73
TL-4	ϵ_1n	S	3.59	−31.6	C_{16}	1.67	0.86	1.37	44.96	0.92	0.45	0.6	28.17	27.78	44.04	0.41	0.35	0.65
TL-5	ϵ_1n	S	8.42	−31.8	C_{16}	1.43	0.69	1.46	18.17	0.7	0.17	0.63	28.42	28.99	42.58	0.41	0.38	0.63
TL-6	ϵ_1n	S	6.64	−31.6	C_{16}	1.89	1.06	1.8	138.39	0.87	0.55	0.61	27.99	29.69	42.32	0.44	0.38	0.65
TL-7	ϵ_1n	S	6.92	−31.6	C_{16}	1.64	1.11	1.65	61.83	0.89	0.44	0.59	30.52	29.47	40.01	0.42	0.38	0.76
TL-8	ϵ_1n	S	7.6	−31.8	C_{16}	1.43	1	2.33	70.75	0.84	0.43	0.59	26.36	29.01	44.64	0.42	0.38	0.58
TL-9	ϵ_1n	S	7.31	−31.8	C_{16}	1.5	1.26	3.42	74.73	0.9	0.32	0.59	26.11	30.11	43.79	0.45	0.4	0.58
TL-10	ϵ_1n	S	8.02	−31.7	C_{16}	2.27	1.93	3.16	102.43	0.75	0.24	0.59	23.74	29.33	46.93	0.46	0.41	0.49
TL-11	ϵ_1n	S	7.95	−31.6	C_{16}	1.78	1.25	2.23	27.54	0.82	0.25	0.62	28.02	28.55	43.43	0.46	0.36	0.66
TL-12	ϵ_1n	S	8.27	−31.8	C_{16}	1.41	1.35	3.3	19.41	0.85	0.37	0.6	28.33	27.7	43.97	0.48	0.37	0.71
TL-13	ϵ_1n	S	8.92	−31.8	C_{16}	1.48	3.62	8.52	7.49	0.96	0.31	0.56	28.3	29.95	41.75	0.48	0.35	0.67
TL-14	ϵ_1n	S	7.57	−31.7	C_{16}	1.43	1.4	3.01	40.64	0.78	0.28	0.64	27.18	29.83	42.99	0.47	0.35	0.67
TL-15	ϵ_1n	S	6.67	−31.7	C_{16}	1.28	0.98	2.01	19.28	0.87	0.19	0.59	28.35	29.65	41.99	0.41	0.35	0.67
TL-16	ϵ_1n	S	7.58	−31.6	C_{16}	1.58	1.53	3.33	16.05	0.91	0.32	0.6	27.94	27.49	44.58	0.44	0.37	0.62
TL-17	ϵ_1n	S	8.11	−31.7	C_{16}	1.6	1.77	3.41	23.5	0.92	0.36	0.6	25.78	29.62	44.6	0.41	0.35	0.56
TL-18	ϵ_1n	S	9.58	−32.0	C_{16}	1.35	2.05	3.71	12.25	1.02	0.15	0.59	27.68	25.31	47.01	0.46	0.41	0.59
TL-19	ϵ_1n	S	9.89	−32.2	C_{16}	1.22	1.27	2.83	42.26	0.99	0.42	0.61	28.57	28.49	42.95	0.39	0.37	0.64
TL-20	ϵ_1n	S	8.14	−31.9	C_{16}	0.85	0.66	1.86	76.43	1.22	0.31	0.6	25.61	28.26	46.13	0.44	0.38	0.53

[a] S = Shale.
[b] C max = n-alkanes with max peak.
[c] C_{21}^{-} = n-alkane with carbon number less than and equal to 21; C_{22}^{+} = n-alkanes with carbon number of 22 and greater.
[d] tt = tricyclic terpane; h = hopane.

4.2. Distributions of the biomarkers

Biomarkers are the organic compounds in sediments, rocks and crude oils whose carbon structure or skeletons can be traced back to a living organism (Hunt, 1996). Marine organic carbon has been found to be composed predominantly of autochthonous phytoplankton (Romankevich, 1984; Hedges and Keil, 1995; and references therein). However, preservation of the organic matter of marine phytoplankton may have occurred when dominantly organic-walled phytoplankton (blue-green algae, acritarchs) were replaced by mainly calcareous-walled organisms (coccolithophorids and dinoflagellates) (Andrusevich et al., 1998). The evolution of biological diversity will also cause some allochthonous terrestrial organic debris to enter younger marine and transitional facies sediments. Thus, the distribution characteristics of biomarkers can be linked to the specific group of plants, animals, or bacteria from which they originated (Hunt, 1996).

4.2.1. n-alkanes

The distribution patterns of *n*-alkanes in typical samples are summarized graphically in Fig. 5. The calculated aliphatic hydrocarbon parameters are listed in Table 3. In all Paleozoic shale samples (from Lower Cambrian to Lower Silurian marine shales), *n*-alkanes are characterized by a higher relative abundance of low-molecular-weight (LMW) homologues and are dominated by C_{16} or C_{17} in most cases. Straight-chain *n*-alkanes from C_{23} to C_{29} display no odd-to-even C number predominance. Most of the analyzed marine shale samples exhibit relatively low Pr/Ph ratios (Pr/Ph range: 0.63–2.27, most less than 1.5). These samples exhibit the typical straight-chain *n*-alkanes distribution characteristics, which indicate that the organic matters in all of the marine shales were sourced from autochthonous phytoplankton (Koopmans et al., 1999) and were in the thermal evolution range of highly mature or post-mature gas-generating stages. Straight-chain *n*-alkanes display a distinct trend of molecular-weight and compound-number reduction with increasing age, suggesting that the organic matter in those shales display an increase in thermal maturity with increased age (burial depth). This finding is confirmed by the variation trend of the contents of soluble organic matter in those marine shales (see above).

4.2.2. Terpenoids

The distribution patterns of terpenoids are summarized graphically in Fig. 6. In nearly all of the analyzed Paleozoic shale samples, tricyclic terpanes are more abundant than hopanes, and the relative abundance of tricyclic terpanes to hopanes show an increasing trend with decreasing age. The maximum peak of tricyclic terpanes also shifts from C_{21} to C_{23} with decreasing age. The tricyclic terpanes are widely distributed in crude oils and source rocks of marine or lacustrine origin and are considered to be diagenetic products of prokaryote membranes (Ourission et al., 1982) and primitive bacteria (Grandville, 1982; Grantham, 1986). Tricyclic terpanes are not usually found in oils predominantly derived from terrestrial source material (Philp and Gilbert, 1986). Hopanoids are the most widespread biomarkers in the biosphere and geosphere and are widely distributed among bacteria, cyanobacteria (blue-green algae) and other primitive organisms with prokaryotic cells (Hunt, 1996). Hopanoids also occur in ferns, lichens and a few higher plants (Ourisson et al., 1982). The concentration of tricyclic terpanes in crude oils appears to increase with increasing maturity, most likely because of the breaking off of tricyclic terpane moieties in asphaltenes and kerogens (Kruge, 1986). Ekweozer and Strauaz (1983) obtained an entire series of homologous tricyclic terpanes in the C_{19}-to-C_{26} range by the pyrolysis of asphaltenes, resins and heavy oils extracted from the Athabasca oil sands of Alberta. The highest yields were obtained from the asphaltenes (Hunt, 1996). Thus, the greater ratio of tricyclic terpanes to hopanes in shale samples suggest that the organic matter in the latter are composed of more terrigenous source material and are less mature.

4.2.3. Steranes

The distribution patterns of steranes are summarized graphically in Fig. 7. The steranes display equal distributions concerning the weak preponderance of C_{27} to C_{29} (Fig. 8). The steranes in the geosphere are presumably derived from sterols in the biosphere. Although sterols have been sporadically reported to occur in prokaryotes (Kohl et al., 1983), it is generally assumed that their contribution to geolipid steranes is minor and that steranes in the geosphere are diagenetically derived mainly from eukaryotes (Demel and Dekruyff, 1976) such as algae, plankton, zooplankton or higher plants (Seifert and Moldowan, 1986). Cholesterol, C_{27}, is the major sterol in 35 species of red algae, and fucosterol, C_{29}, was dominant in all brown algae examined (Patterson, 1971). The

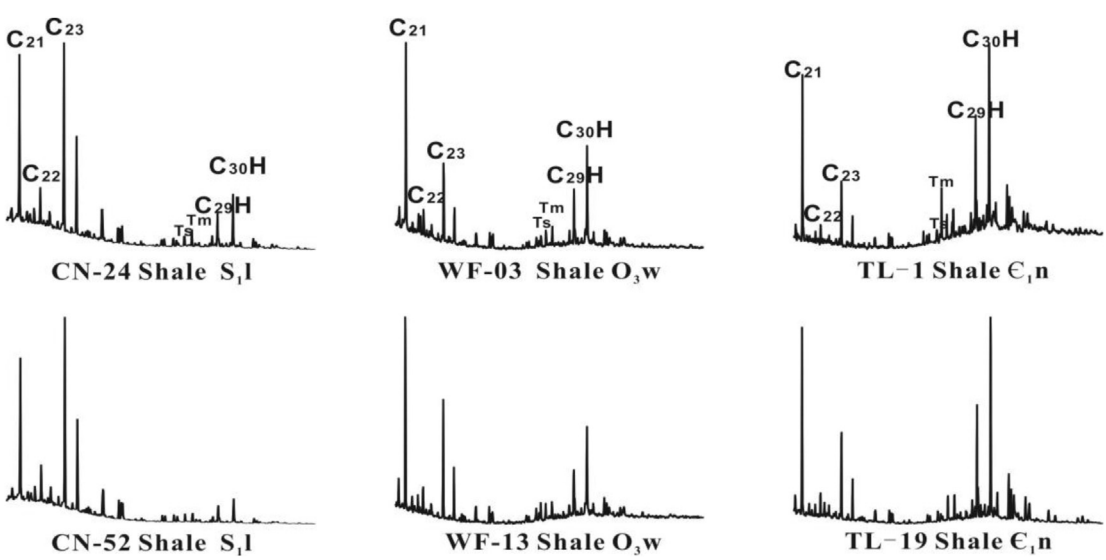

Fig. 6. Comparison of the distributions of terpenoids in different strata.

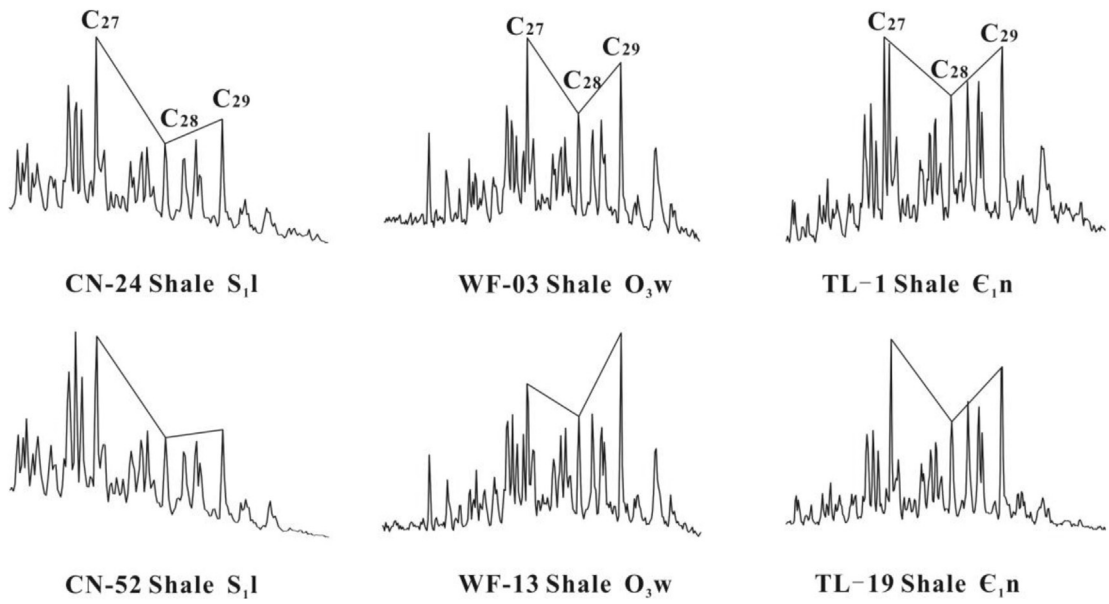

Fig. 7. Comparison of the distributions of steranes in different strata.

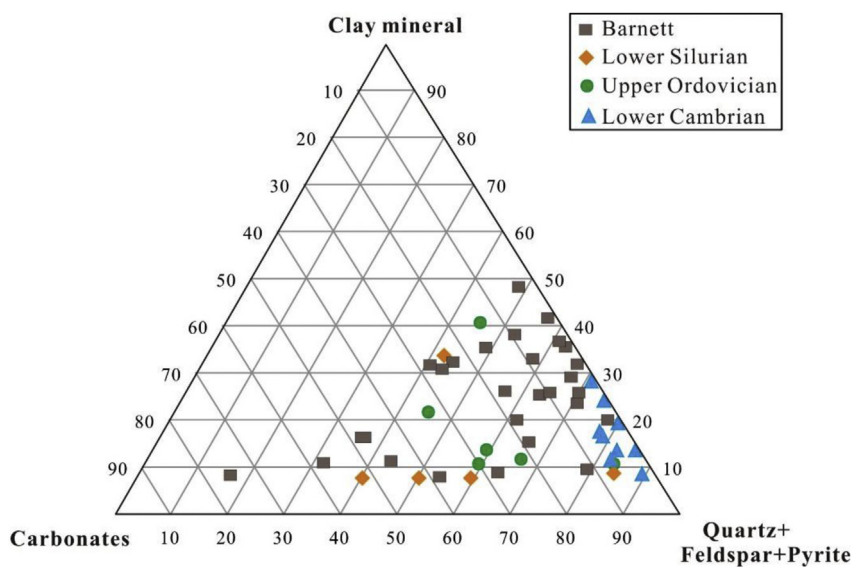

Fig. 8. Ternary diagram showing a comparison of the mineralogical constituents of Paleozoic marine shales examined in this study with those of Barnett shales (data regarding Barnett shales were obtained from Loucks and Ruppel, 2007).

sterols of green algae are more complex. Ergosterol, C_{28}, was predominant in five species of *Chlorella*. In five other species, chondrillasterol, C_{29}, was the major sterol (Patterson, 1971). The major sterol in higher plants is β-sitosterol, C_{29}. Stigmasterol, C_{29}, is abundant in soybeans and other terrestrial plants. Campesterol, C_{28}, and brassicastreol, C_{28}, are other sterols found in land plants. None of these four sterols are an important constituent of marine or lacustrine organisms (Hunt, 1996).

4.3. Mineralogy and petrophysical characteristics

We selected 20 lower Paleozoic marine shale samples for X-ray diffraction analyses and porosity and pore structure analyses to further evaluate the porosity, pore size distribution and total gas capacity in the lower Paleozoic marine shales.

4.3.1. Mineralogical constituents and brittleness index

Mineralogy is a key factor characterizing the best shale gas wells (Bowker, 2003a). The measured mineralogical constituents for the 20 selected (depending mainly on the variation of TOC contents) lower Paleozoic marine shale samples (six for Lower Silurian, five for Upper Ordovician and nine for Lower Cambrian) are listed in Table 4. On average, the Lower Cambrian Niutitang Formation shales contain more quartz (52–69%) than the Lower Silurian (32–60%) and Upper Ordovician shales (34–78%). The quartz contents in the Lower Silurian shale display a distinct increasing trend (from 32% to 60%) with increasing age. The Upper Ordovician shales contain smaller amounts of quartz but relatively greater amounts of calcite and dolomite than the Lower Cambrian and Lower Silurian shales. Lower Cambrian shales contain relatively greater amounts of plagioclase, pyrite and clay mineral than the Lower Silurian and

Table 4
TOC, Mineral compositions, and brittleness index (BI) for the 3 lower Paleozoic marine strata (%).

Strata	Sample no.	TOC	Quartz	Calcite	Dolomite	Plagioclase	Pyrite	Microcline	Clay mineral	BI_1	BI_2
Lower Silurian	CN-66	1.17	32	28	5	5	1	7	22	39.0	42.0
	CN-25	1.56	36	10	4	4	4	2	41	41.4	43.2
	CN-17	3.98	54	7	20	3	1	nd	14	72.0	74.8
	CN-11	3.42	54	17	13	2	1	2	11	65.9	68.1
	CN-02	7.13	79	3	3	1	2	nd	11	84.9	79.5
	CN-01	5.45	60	14	8	4	2	nd	12	69.8	68.4
Upper Ordovician	WF-19	7.76	78	3	4	3	1	nd	9	86.7	80.6
	WF-14	4.81	34	22	30	4	3	nd	8	53.1	64.8
	WF-12	3.46	48	35	7	1	2	nd	8	52.7	54.2
	WF-08	2.36	58	22	11	1	1	nd	8	65.9	68.1
	WF-01	1.18	34	6	18	5	nd	3	34	45.9	55.8
Lower Cambrian	TL-3	2.92	60	nd	nd	6	3	2	29	67.4	65.3
	TL-4	3.59	58	nd	nd	7	7	2	25	69.9	67.0
	TL-5	8.42	59	nd	nd	9	11	1	20	74.7	67.5
	TL-7	6.92	61	nd	5	9	6	1	18	77.2	72.6
	TL-11	7.95	64	nd	4	9	7	2	14	82.1	75.6
	TL-13	8.92	61	nd	6	9	10	2	12	83.6	76.2
	TL-16	7.58	52	nd	5	15	9	3	17	75.4	69.9
	TL-18	9.58	68	nd	2	7	12	2	9	88.3	79.0
	TL-19	9.89	69	nd	nd	7	9	1	14	83.1	74.3

$BI_1 = \frac{Qz}{Qz+Ca+Clay}$(Jarvie et al., 2007), $BI_2 = \frac{Qz+Dol}{Qz+Ca+Clay+Dol+TOC}$(Wang and Gale, 2009).
Qz: Quartz, Ca: calcit content, Dol: dolomite content, nd: no detected.

Upper Ordovician shales. In the comparative diagram of the strata demonstrating the proximal vertical variation in the mineralogical constituents and TOC content (Fig. 9a, b), the quartz and the TOC show strong agreement in terms of their contents (Fig. 10a). This finding strongly suggests that the increasing quartz content in the Lower Cambrian Niutitang Formation, the upper parts of the Upper Ordovician Wufeng Formation and the lower parts of Lower Silurian Longmaxi Formation is an indicator of biogenic silica. Furthermore, the relatively greater level of biogenic silica debris deposited synchronously led to a greater TOC content in the marine sediment.

The ternary diagram comparing the mineralogical composition of the Paleozoic marine shales examined in this study with that of Barnett shales displays the relative proportions of clay, carbonate and other minerals (Fig. 8). All of the Paleozoic marine shales analyzed (from the Lower Cambrian to Lower Silurian marine shales) are plotted within the area of the Barnett shales. Brittleness is a key parameter in evaluating shale fracturing. Since different minerals have different brittleness, the rock higher in brittle mineral content is also higher in brittleness. Mineral brittleness index (BI), is one the important parameters for screening shale-gas systems, Sichuan Basin are favorable for fracturing production for shale gas. Brittleness index of Paleozoic shales in Sichuan Basin were characterized by Jarvie et al.'s (2007) and Wang and Gale's (2009) equations (Table 4). All Paleozoic organic rich shales with TOC greater than 2.0% exhibit high BI, higher than 50%. High level of brittle mineralogical constituents and brittleness index suggest that the Paleozoic marine shales in the Sichuan Basin are favorable for shale gas production which can be accomplished economically only with horizontal drilling and hydraulic fracturing.

4.3.2. Porosity and pore size distribution

The characteristics of pores (pore volume and pore size distribution) with overmature organic-rich formations may provide some insight into how they function and the mechanism responsible for their formation. The measured total porosities for the 20

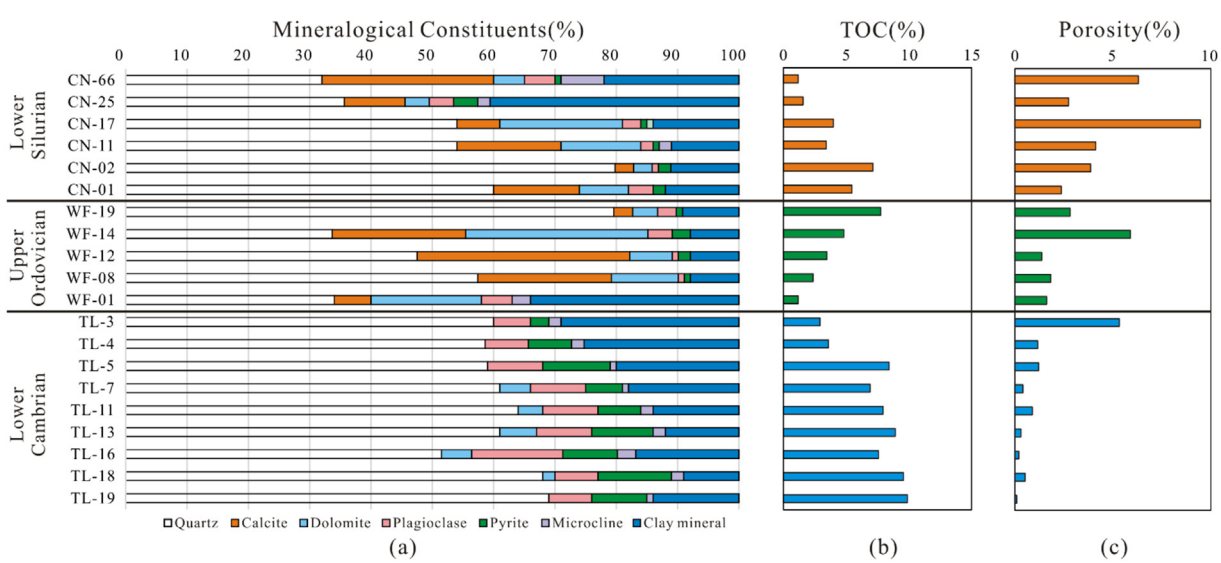

Fig. 9. Comparative diagram of strata expressed in terms of proximal vertical variation: (a) mineralogical constituents, (b) TOC (%), (c) porosity (%).

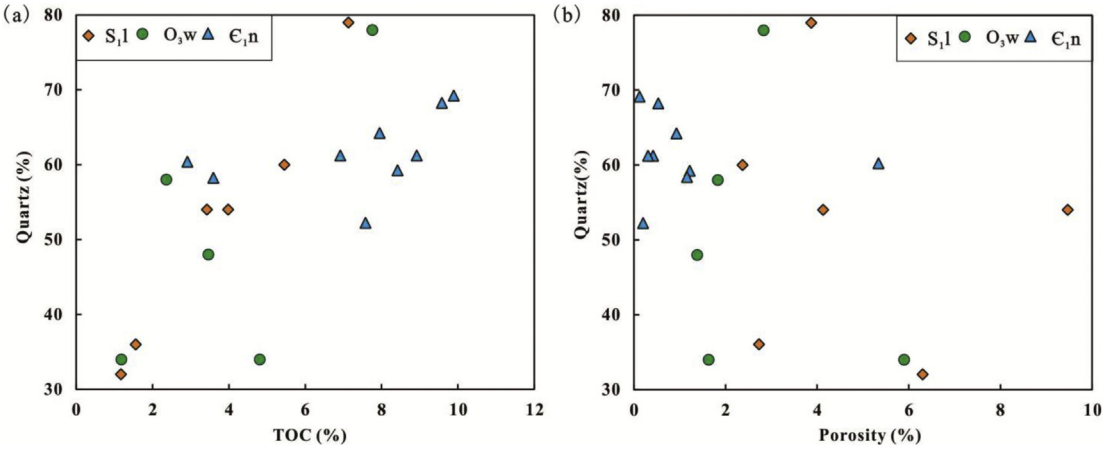

Fig. 10. Plots of TOC and porosity versus quartz.

selected lower Paleozoic marine shale samples are graphically illustrated and compared vertically with the variation in TOC and mineralogical constituents in Fig. 9. The total porosity for most of the analyzed samples was less than 5%. Vertically, the total porosity displays a roughly decreasing trend with increasing age (Fig. 9c). The total porosities in the six Lower Silurian marine shales ranged from 2.4% to 9.5%, those in the five Upper Ordovician shales ranged from 1.6% to 5.9%, and those in the nine Lower Cambrian shales were nearly all less than 2.0% (expect for one sample at 5.3%). The total porosity displays a roughly negative relationship with the TOC and quartz contents in the vertical diagram (Figs. 9 and 10b). The pore size distributions also display significant differences between different marine shale strata (Fig. 11). The Lower Cambrian shales have pore sizes skewed toward smaller pores and lower total pore volumes, most notably pore sizes with a distribution range of less than 50 nm (micropores and mesopores), whereas in the Lower Silurian shales, the pores are almost uniformly distributed over different pore sizes (micropores, mesopores and macropores). In the Upper Ordovician shales, the pores were mainly composed of micropores and mesopores with small amounts of macropores (Fig. 11). FE-SEM imaging results was in line with porosity and pore diameter analytical results (Fig. 12). Compared to the Cambrian shale, organic-matter pores widely distributed in the Lower Silurian shales. These findings are in contrast to those of other studies that indicate increasing porosity with quartz content and TOC due to the presence of intergranular pores between coarser detrital grains (Schlömer and Krooss, 1997; Dewhurst et al., 1999) and that porosity was created by organic matter decomposition (Jarvie et al., 2007; Chen and Xiao, 2014).

In previous shale gas studies, sorbed CH_4 capacities were correlated with TOC (Manger et al., 1991; Lu et al., 1995; Ross and Bustin, 2007; Zhang et al., 2012). Chalmers and Bustin (2007) reported an increase in CH_4 sorption capacity with an increase in micropore volume for Cretaceous shales, similarly to results reported for coalbed methane reservoirs (Lamberson and Bustin, 1993; Crosdale et al., 1998; Clarkson and Bustin, 1999). Microporosity, which is positively correlated with TOC in shales (Chalmers and Bustin, 2007), is a critical component of porous media because of the large internal surface areas and greater sorption energies of sub-2-nm pores compared with larger pores of solids with similar composition (Dubinin, 1975). Porosity is observed at the microscale in organics, between grains, in pyrite framboids, in fossils, within minerals and in the form of microcracks. The majority of pores in some shales are located in organic matter. Other shales indicate that porosity is largely associated with minerals (Sondergeld et al., 2010). Jarvie et al. (2007) propose an average TOC content of

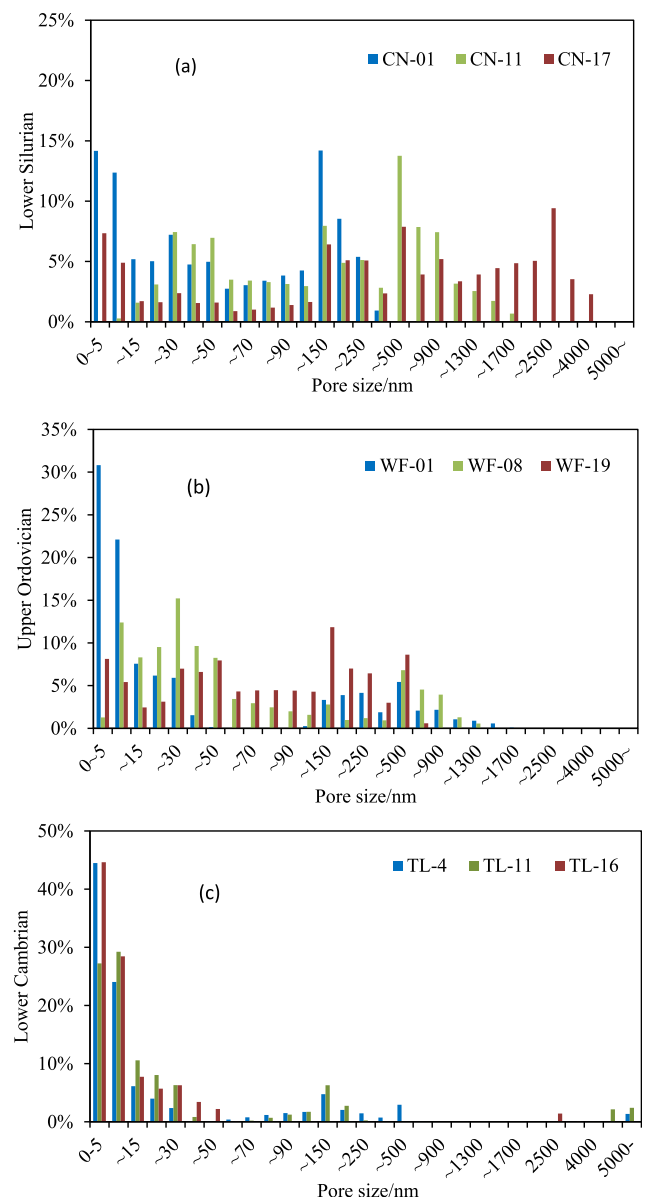

Fig. 11. Comparison of the pore size distributions in different marine shales in the Sichuan Basin: (a) Lower Silurian, (b) Upper Ordovician, (c) Lower Cambrian.

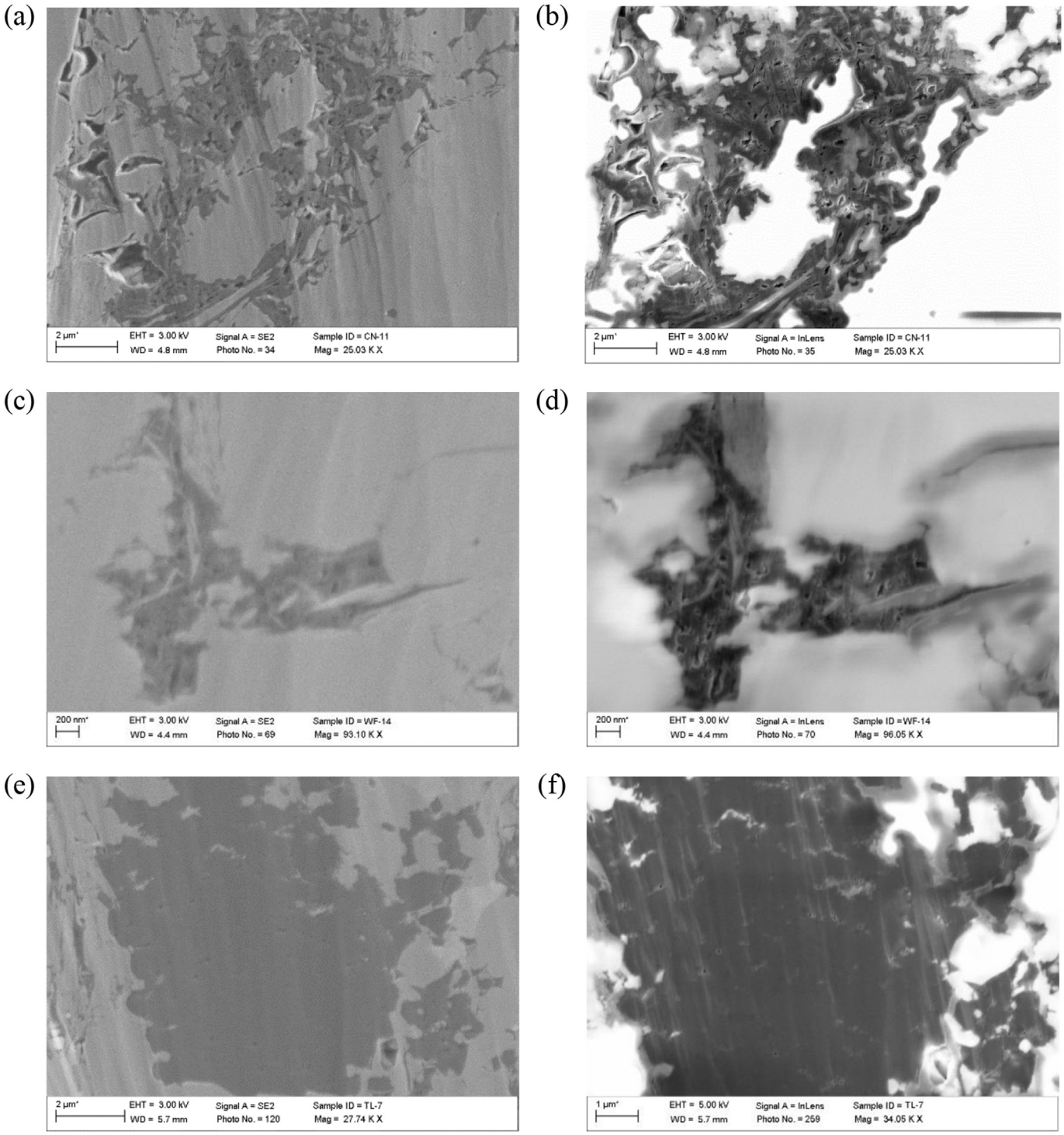

Fig. 12. Field emission scanning electron microscope (FE-SEM) images of organic-matter pores in different marine shales in the Sichuan Basin: (a) (b) Lower Silurian, (c) (d) Upper Ordovician, (e) (f) Lower Cambrian.

6.41 wt. % (mass), with a volume percent TOC of approximately 12.7 vol. % using a density of 1.18 g/cm^3 for organic matter. When thermal maturation is in the dry-gas window (e.g., >1.4% Ro), approximately 4.3 vol. % porosity is created by organic matter decomposition. In such a case, we would expect at least 4.5% porosity in the Lower Cambrian shales, created by organic matter decomposition alone, because nearly all of the samples contained >7% sapropelic oil-prone TOC. A previous study indicates that much of the oil generated in sedimentary rocks remains disseminated in fine-grained source rocks, and the ratio of oil in nonreservoir rocks to that in reservoirs for all rocks is approximately 200 to 1. In basins with large oil fields, the ratio may range from 20 to 50 to 1 (Hunt, 1996). The maximum percent of TOC converted to C in oil can be 58% and 42% for sapropelic type I and type II kerogens, respectively, 31% and 26% of which can convert to gas if all of the previously formed oil is converted to gas (Hunt, 1996). That is, approximately 27% and 16% of the TOC will be reassembled as pyrobitumen (coke) for sapropelic type I and type II kerogens, respectively, when

previously formed oil is cracked to gas in overmature source rocks. The re-precipitated pyrobitumen (coke) causes the previously created pores to be filled again. Oil cracking to gas in overmature source rocks can occur in both intergranular pores and the pores in organic matter created previously by organic matter decomposition, and the cracking can cause the pore volume to decrease and the pore sizes to skew toward smaller pores. These processes are most likely the main reasons why we only obtained the lowest porosity and minimum pore sizes in the most aged but most TOC-abundant Lower Cambrian shales. This porosity and pore-size reduction phenomenon in overmature source rock via re-precipitation of pyrobitumen created by oil cracked to gas requires further confirmation by visual observation in future research. Both the volume and sizes skewing toward smaller pores in overmature higher TOC shales appears to be an unusual finding, one that has not been, to the best of our knowledge, previously reported. Because skewing toward smaller pores will reduce the pore volume, increase the internal surface area and increase the sorption energy compared with those of larger pores of solids with similar composition, the shale gas storage space will be reduced, and a relatively greater amount of gas will occur as adsorbed gas in overmature, high-TOC shale, which will lower the productive capacity of shale gas.

5. Conclusions

(1) Lower Cambrian, Upper Ordovician, and Lower Silurian in the Sichuan Basin all displayed excellent, high-quality organic matter richness features and could be the strata that have supported shale gas generation over geological time. The measured $\delta^{13}C$ value for the sedimentary organic carbon in the three black shale strata in the Sichuan Basin present a distinct trend of ^{13}C enrichment, indicating that TOC may be related to the diversity of preserved phytoplankton in the different shale strata in the Sichuan Basin. The light $\delta^{13}C$ values of the TOC in the Lower Paleozoic marine shales suggest that the organic matter in those shale strata were sapropelic, oil-prone materials.

(2) Biomarker distribution characteristics suggest that the organic matter in the marine shales were mainly composed of autochthonous marine phytoplankton. The bitumen "A" content displays a negative correlation with sedimentary age and TOC, suggesting that most of the residual liquid hydrocarbons in those shales have been transformed into shale gas due to higher thermal maturity during the diagenetic transformation of the organic matter burial process, and the shale gas stored in reservoirs in those types of shales was mostly generated from the cracking of residual bitumen during a stage of relatively high thermal evolution.

(3) All of the measured Paleozoic marine shales were favorable for the fracturing production of shale gas, similarly to Barnett shale, with a relatively high level of brittle mineralogical constituents. The negative relationship observed between the total porosity and the TOC and quartz contents in the three Paleozoic marine shales suggests that re-precipitated pyrobitumen (coke) created by oil cracked to gas in overmature source rocks may have led to the lowest porosity level and minimum pore sizes in the most aged but most TOC-abundant shales. Because skewing toward smaller pores reduces the pore volume, increases the internal surface area and increases sorption energies compared with those of the larger pores of solids with similar composition, the shale gas storage space will be reduced, and a relatively greater amount of gas will occur as adsorbed gas in overmature, higher-TOC shale, which will lower the productive capacity of shale gas.

Acknowledgments

This research was supported by the National Programs for Fundamental Research and Development of China (973 Program) (Grant No.2012CB214701), the CAS Action-Plan for West Development (Grant No.KZCX2-XB3-12), and the Key Laboratory Project of Gansu Province (Grant No.1309RTSA041). We thank two anonymous reviewers who refereed this paper and the Editor-in-Chief David A. Wood for all their valuable comments that helped to greatly improve the quality of the paper.

References

Andrusevich, V.E., Engel, M.H., Zumberge, J.E., Brothers, L.A., 1998. Secular, episodic changes in stable carbon isotope composition of crude oils. Chem. Geo 152, 59–72.
Arthur, M.A., Dean, W.E., Pratt, L.M., 1985. Geochemical and climatic effects of increased marine organic carbon burial at the cenomanian/turonian boundary. Nature 335, 714–717.
Bowker, K.A., 2003a. Recent development of the barnett shale play, fort Worth Basin. West Tex. Geol. Soc. Bull. 42, 1–11.
Chalmers, G.R.L., Bustin, R.M., 2007. The organic matter distribution and methane capacity of the lower cretaceous strata of northeastern British Columbia. Int. J. Coal Geol. 70, 223–239.
Chen, J., Xiao, X., 2014. Evolution of nanoporosity in organic-rich shales during thermal maturation. Fuel 129, 173–181.
Chen, S., Zhu, Y., Fang, H., Liu, H., Wei, W., Fang, J., 2011. Shale gas reservoir characterisation: a typical case in the southern Sichuan Basin of China. Energy 36, 6609–6616.
Clarkson, C.R., Bustin, R.M., 1999. The effect of pore structure and gas pressure upon the transport properties of coal: a laboratory and modeling study. 1. Isotherms and pore volume distributions. Fuel 78, 1333–1344.
Crosdale, P.J., Beamish, B.B., Valix, M., 1998. Coalbed methane sorption related to coal composition. Int. J. Coal Geol. 35, 147–158.
Curtis, J.B., 2002. Fractured shale-gas systems. AAPG Bull. 86, 1921–1938.
Dai, J., Xia, X., Wei, Y., Tao, Z., 2001. Carbon isotope characteristics of natural gas in the Sichuan Basin, China. Petro. Geol. Exper. 23, 115–132 (in Chinese with English abstract).
Dai, J., Zou, C., Liao, S., Dong, D., Ni, Y., Huang, J., et al., 2014. Geochemistry of the extremely high thermal maturity Longmaxi shale gas, southern Sichuan Basin. Org. Geochem. 74, 3–12.
Dawson, T.E., Mambelli, S., Plamboeck, A.U., Templer, P.U., Tu, K.P., 2002. Stable isotopes in plant ecology. Ann. Rev. Eco. Syst. 33, 507–559.
Dean, W.E., Arthur, M.A., Claypool, G.E., 1986. Depletion of ^{13}C in Cretaceous marine organic matter: source, diagenetic, or environmental signal? Mar. Geol. 70, 119–157.
Demel, R.A., Dekruyff, B., 1976. The function of sterols in membranes. Biochem. Biophys. Acta. 457, 109–132.
Dewhurst, D.N., Yang, Y., Aplin, A.C., 1999. Permeability and fluid flow in natural mudstones. In: Aplin, A.C., Fleet, A.J., Macquaker, J.H.S. (Eds.), Muds and Mudstones. Physical and Fluid Flow Publications, pp. 125–136.
Dubinin, M.M., 1975. Physical adsorption of gases and vapours in micropores. In: Cadenhead, D.A., Danielli, J.F., Rosenberg, M.D. (Eds.), Progress in Surface and Membrane Science, vol. 9. Academic Press, New York, pp. 1–70.
Edwards, D., Davies, K.L., Axe, L.M., 1992. A vascular conducting strand in the early land plant. Cooksonia. Nat. 357, 683–685.
Ekweozor, C.M., Strausz, O.P., 1983. Tricyclic terpanes in the athabasca oil sands: their geochemistry. In: Bjorøy, et al. (Eds.), Advances in Organic Geochemistry 1981. Wiley, Chichester, pp. 746–766.
De la Grandville, B.F., 1982. Appraisal and development of a structural and stratigraphic trap oil field with reservoir in glacial to periglacial clastics. In: Halbouty, M.T. (Ed.), The Deliberate Search for the Subtle Trap. AAPG Memoir 32American Association of Petroleum Geologists, Tulsa, pp. 267–286.
Grantham, P.L., 1986. The occurrence of unusual C_{27} and C_{29}sterane predominance in two types of Oman crude oil. Org. Geochem 9, 1–10.
Hao, F., Zhou, H., 2013. Cause of shale gas geochemical anomalies and mechanisms for gas enrichment and depletion in high-maturity shales. Mar. Petrol. Geol. 44, 1–12.
Hao, F., Zhou, H., Lu, Y., 2013. Mechanisms of shale gas storage: Implications for shale gas exploration in China. AAPG Bull. 97, 1325–1346.
Hayes, J.M., Popp, B.N., Takigiku, R., Johnson, M.W., 1989. An isotopic study of biogeochemical relationships between carbonates and organic carbon in the Greenhorn Formation. Geochim. Cosmochim. Acta 53, 2961–2972.
Hedges, J.I., Keil, R.G., 1995. Sedimentary organic matter preservation: an assessment and speculative synthesis. Mar. Chem. 49, 81–115.
Hill, R.J., Jarvie, D.M., Zumberge, M., Henry, J., Pollastro, R.M., 2007. Oil and gas geochemistry and petroleum systems of the Fort Worth Basin. AAPG Bull. 91,

445–473.
Huang, J., Chen, S., Song, J., Wang, L., Gou, X., Wang, T., Dai, H., 1996. Hydrocarbon source systems and formation of gas fields in Sichuan Basin. Sci. China Ser. D 26, 504–510 (in Chinese with English abstract).
Hunt, J.M., 1996. Petroleum Geochemistry and Geology, second ed. Freeman and Company, New York.
Jarvie, D.M., Hill, R.J., Ruble, T.E., Pollastro, R.M., 2007. Unconventional shale-gas systems: the Mississippian Barnett Shale of north-central Texas as one model for thermogenic shale-gas assessment. AAPG Bull. 91, 475–499.
Kaufman, A.J., Hayes, J.M., Knoll, A.H., Germs, G.J.B., 1991. Isotopic compositions of carbonates and organic carbon from upper Proterozoic successions in Namibia: stratigraphic variation and the effect of diagenesis and metamorphism. Precambrian Res. 49, 301–327.
Kenrick, P., Crane, P.R., 1997. The origin and early evolution of plants on land. Nature 389, 33–39.
Knoll, A.H., Hayes, J.M., Kaufman, A.J., Sweet, K., Lambert, I.B., 1986. Secular variations in carbon isotope ratios from Upper Proterozoic successions of Svalbard and East Green-land. Nature 321, 832–838.
Kodina, L.A., Galimov, E.M., 1985. Origin of carbon isotope compositions in organic matter of humic and sapropelic types in marine sediments. Geochem. Int. 22, 87–100.
Kohl, W., Gloc, A., Reichenbach, H., 1983. Steroids from one Myzobacterium Nannocystisexedens. J. Gen. Microboil. 129, 1624–1635.
Koopmans, M.P., Rijpstra, W.I.C., Klapwijk, M.M., de Leeuw, J.W., Lewan, M.D., Sinninghe Damste', J.S., 1999. A thermal and chemical degradation approach to decipher pristine and phytane precursors in sedimentary organic matter. Org. Geochem. 30, 1089–1104.
Kruge, M.A., 1986. Biomarkers geochemistry of the Miocene Monterey formation, west San Joaquin Basin, California: Implications for petroleum generation. Org. Geochem. 10, 517–530.
Lamberson, M.N., Bustin, R.M., 1993. Coalbed methane characteristics of Gates formation coals, northeastern British Columbia: effect of maceral composition. AAPG Bull. 77, 2062–2076.
Liang, D., Guo, T., Chen, J., Bian, L., Zhao, Z., 2009. Some progresses on studies of hydrocarbon generation and accumulation in marine sedimentary regions, southern China (Part 1): distribution of four suits of regional marine source rocks. Mar. Orig. Petrol. Geol. 14, 1–16 (in Chinese with English abstract).
Loucks, R.G., Ruppel, S.C., 2007. Mississippian Barnett Shale: Lithofacies and depositional setting of a deep-water shale-gas succession in the Fort Worth Basin, Texas. AAPG Bull. 91, 579–601.
Lu, X., Li, F., Watson, A.T., 1995. Adsorption measurements in Devonian shales. Fuel 74, 599–603.
Ma, L., Chen, H., Gan, K., Xu, K., Xu, X., Wu, G., Ye, Z., 2004. Geostructure and Marine Facies Hydrocarbon Geology of South China, Volume one. Geological Publishing House, Beijing, pp. 259–364 (in Chinese with English abstract).
Manger, K.C., Oliver, S.J.P., Curtis, J.B., Scheper, R.J., 1991. Geologic Influences on the Location and Production of Antrim Shale Gas, Michigan Basin, pp. 511–519. SPE 21854.
Nie, H., Tang, X., Bian, R., 2009. Controlling factors for shale gas accumulation and prediction of potential development area in shale gas reservoir of South China. Acta Pet. Sin. 30, 484–491 (in Chinese with English abstract).
Nie, H., Zhang, J., Li, Y., 2011. Accumulation conditions of the Lower Cambrian shale gas in the Sichuan Basin and its periphery. Acta Pet. Sin. 32, 959–967.
Ourisson, G., Albrecht, P., Rohmer, M., 1982. The microbial origin of fossil fules. Sci. Am. 251, 44–51.
Patterson, G.W., 1971. The distribution of sterols in algae. Lipids 6, 120–126.
Philp, R.P., Gilbert, T.D., 1986. Biomarker distributions in Australian oils predominantly derived from terrigenous source material. Org. Geochem 10, 73–84.
Popp, B.N., Parekh, P., Tilbrook, B., Bidigare, R.R., Laws, E.A., 1997. Organic carbon $\delta^{13}C$ variations in sedimentary rocks as chemostratigraphic and paleoenvironmental tools. Palaeogeogr. Palaeoclim. Palaeoecolo. 132, 119–132.
Romankevich, E.A., 1984. Geochemistry of Organic Matter in the Ocean. Springer, Berlin, p. 334.
Ross, D.J.K., Bustin, R.M., 2007. Shale gas potential of the lower Jurassic Gordondale Member, northeastern British Columbia, Canada. Bull. Can. Petrol. Geol. 55, 51–75.
Schlömer, S., Krooss, B.M., 1997. Experimental characterisation of the hydrocarbon sealing efficiency of cap rocks. Mar. Petrol. Geol. 14, 565–580.
Seifert, W.K., Moldowan, J.M., 1986. Use of biological markers in petroleum exploration. In: Johns, R.B. (Ed.), Biological Markers in the Sedimentary Record. Elsevier, Amsterdam, pp. 261–290.
Sondergeld, C.H., Ambrose, R.J., Rai, C.S., Moncrieff, J., 2010. Micro-structural Studies of Gas Shales, pp. 1–17. SPE 131771.
Strąpoć, D., Mastalerz, M., Schimmelmann, A., Drobniak, A., Hasenmueller, N.R., 2010. Geochemical constraints on the origin and volume of gas in the New Albany Shale (Devonian–Mississippian), eastern Illinois Basin. AAPG Bull. 94, 1713–1740.
Tenger, Gao, C., Hu, K., Fang, C., Lv, J., Zhai, C., Zhang, C., 2007. High quality source rocks of lower combination in the northern Upper-Yangtze area and their hydrocarbon potential. Nat. Gas. Geosci. 18, 254–259 (in Chinese with English abstract).
Tissot, B., Welte, D.H., 1984. Petroleum Formation and Occurrence, Seconded. Springer-Verlag, New York.
Wang, F., Gale, J., 2009. Screening criteria for shale-gas systems. GCAGS Trans. 59, 779–793.
Wang, L., Zou, C., Zheng, P., Chen, S., Zhang, Q., Xu, B., Li, H., 2009. Geochemical evidence of shale gas existed in the Lower Paleozoic Sichuan Basin. Nat. Gas. Ind. 29, 59–62 (in Chinese with English abstract).
Xia, X., 2014. Kinetics of gaseous hydrocarbon generation with constraints of natural gas composition from the Barnett Shale. Org. Geochem 74, 143–149.
Xia, X., Chen, J., Braun, R., Tang, Y., 2013. Isotopic reversals with respect to maturity trends due to mixing of primary and secondary products in source rocks. Chem. Geo. 339, 205–212.
Zhang, D., Zhang, J., Li, Y., Qiao, D., Jiang, W., 2011. Shale Gas Potential Assessment and Selection of Favorite Exploration Areas in China (in Chinese). RCOGR (Research Center of Oil and Gas Resources of the Ministry of Land and Resources). Research Report, 117.
Zhang, J., Nie, H., Xu, B., Jiang, S., Zhang, P., Wang, Z., 2008. Geology conditions of shale gas accumulation in Sichuan Basin. Nat. Gas. Ind. 28, 151–156 (in Chinese with English abstract).
Zhang, J., Jin, Z., Yuan, M., 2004. Reservoiring mechanism of shale gas and its distribution. Nat. Gas. Ind. 24, 14–18 (in Chinese with English abstract).
Zhang, T., Ellis, G.S., Ruppel, S.C., Milliken, K., Yang, R., 2012. Effect of organic-matter type and thermal maturity on methane adsorption in shale-gas systems. Org. Geochem. 47, 120–131.
Zhang, T., Yang, R., Milliken, K.L., Ruppel, S.C., Pottorf, R.J., Sun, X., 2014. Chemical and isotopic composition of gases released by crush methods from organic rich mud rocks. Org. Geochem. 73, 16–28.
Zhou, Q., Xiao, X., Tian, H., Pan, L., 2014. Modeling free gas content of the Lower Paleozoic shales in the Weiyuan area of the Sichuan Basin, China. Mar. Petrol. Geol. 56, 87–96.
Zhu, G., Zhang, S., Liang, Y., 2006. The characteristics of natural gas in Sichuan Basin and its sources. Earth Sci. Front. 13, 234–248 (in Chinese with English abstract).
Zhu, Y., Chen, S., Fang, J., Luo, Y., 2010. The geologic background of the Siluric shale-gas reservoiring in Sichuan, China. J. China Coal Soci. 35, 1160–1164 (in Chinese with English abstract).
Zou, C., Wei, G., Xu, C., Du, J., Xie, Z., Wang, Z., Hou, L., Yang, C., Li, J., Yang, W., 2014. Geochemistry of the Sinian-Cambrian gas system in the Sichuan Basin, China. Org. Geochem. 74, 13–21.
Zou, C., Dong, D., Wang, S., Li, J., Li, X., Wang, Y., Li, D., Cheng, K., 2010. Geological characteristics and resource potential of shale gas in China. Petrol. explor. Dev. 37, 641–653.
Zou, C., Yang, Z., Dai, J., Dong, D., Zhang, B., Wang, Y., et al., 2015. The characteristics and significance of conventional and unconventional Sinian–Silurian gas systems in the Sichuan Basin, central China. Mar. Petrol. Geol. 64, 386–402.